

## Interlayer structure, anion dynamics, and phase transitions in mixed-metal layered hydroxides: Variable temperature $^{35}\text{Cl}$ NMR spectroscopy of hydrotalcite and Ca-aluminate hydrate (hydrocalumite)

R. JAMES KIRKPATRICK,<sup>1,3,\*</sup> PING YU,<sup>2,3</sup> XIAOQIANG HOU,<sup>1</sup> AND YEONGKYOON KIM<sup>1,†</sup>

<sup>1</sup>Department of Geology, University of Illinois at Urbana-Champaign, 1301 W. Green Street, Urbana, Illinois 61801, U.S.A.

<sup>2</sup>Department of Materials Science and Engineering, University of Illinois at Urbana-Champaign, Urbana, Illinois 61801, U.S.A.

<sup>3</sup>National Science Foundation Center for Advanced Cement-Based Materials, University of Illinois at Urbana-Champaign, Urbana, Illinois 61801, U.S.A.

### ABSTRACT

The  $^{35}\text{Cl}$  NMR spectroscopy of  $\text{Cl}^-$ -intercalated hydrotalcite and the Ca-aluminate hydrate hydrocalumite (Friedel's salt) demonstrates dynamical behavior of interlayer  $\text{Cl}^-$ , the presence of dynamical order-disorder phase transitions in these phases, and significant differences in the transition temperatures and temperature interval over which the transitions occur. In hydrocalumite, the Ca,Al distribution is ordered, the interlayer water is directly coordinated to Ca in the hydroxide layer (creating sevenfold-coordinated Ca), and the interlayer  $\text{Cl}^-$  and water sites are well ordered. The  $^{35}\text{Cl}$  NMR data show that the interlayer  $\text{Cl}^-$  site has uniaxial or nearly uniaxial symmetry above about  $0^\circ\text{C}$  and reduced (triaxial) symmetry at lower temperatures. Differential scanning calorimetry (DSC) data show this change to be due to a structural phase transition at about  $6^\circ\text{C}$ . The NMR and XRD data suggest that this phase transition is due to dynamical order-disorder involving a rigid interlayer atomic arrangement at low temperatures and dynamically averaged interlayer species at high temperatures. In contrast, in hydrotalcite Mg and Al are disordered over the octahedral sites, and the interlayer is disordered. The  $^{35}\text{Cl}$  NMR data for it show poorly resolved signal indicating a range of  $\text{Cl}^-$  environments and a change from triaxial to uniaxial or nearly uniaxial symmetry at  $\text{Cl}^-$  occurring over a broad temperature interval below  $-40^\circ\text{C}$ . DSC data for our sample shows a broad and poorly defined endothermic anomaly in the  $-100$  to  $-75^\circ\text{C}$  range. These data suggest the presence of a phase transition that occurs over a larger temperature range due to its disordered interlayer structure. The results suggest that similar variable temperature NMR behavior previously observed for interlayer cations in smectites can be thought of as due to comparable phase transitions that lack well-defined critical temperatures due to the disordered interlayer structures.

### INTRODUCTION

Mixed-metal layered hydroxides (MMLHs) are among the few oxide-based materials that exhibit substantial, permanent anion exchange capacity due to isomorphic substitution, and hydrotalcite-like compounds have been often suggested as anion exchange materials for environmental remediation (Miyata 1983; Parker et al. 1995; Wada and Masuda 1995; Pinnavaia 1995; Ulbarri et al. 1995; Amin and Jayson 1996; Hermosin et al. 1996; Olguin et al. 1998). Ca-based MMLHs are also important phases in Ca-silicate and Ca-aluminate cement systems, where they play an anion binding role and can also play an important structural role (Taylor 1997). Use of the Ca-based MMLHs for environmental applications has not been well investigated, but like hydrotalcite they may be useful. As for many

silicate-based clay minerals, the structural environments and dynamical behavior of the interlayer species in MMLHs are difficult to study and poorly understood, and NMR spectroscopy is likely to be an effective probe of both (e.g., Kim et al. 1996 and references therein). For interlayer species in MMLHs, NMR has been used only for  $^{13}\text{C}$  and  $^1\text{H}$  in hydrotalcite (Marcelin et al. 1989; van der Pol et al. 1994), although many anionic species can be observed. We report here the first  $^{35}\text{Cl}$  NMR study of MMLHs, with emphasis on the contrasting behavior of interlayer chloride in hydrotalcite-like compounds (known as HTs, here molar  $\text{Mg}/(\text{Mg}+\text{Al}) = 0.75$ ) and the layered Ca-aluminate MMLH, hydrocalumite (also known as Friedel's salt; nominally  $\text{Ca}_2\text{Al}(\text{OH})_6\text{Cl}\cdot 2\text{H}_2\text{O}$ ). Layered Ca-aluminate hydrates are known collectively as AFm phases in the cement science literature (after the Al,Fe,Ca-mono-sulfate compound), and we use that term here. In nature, hydrocalumite is a  $\text{Cl}^-,\text{OH}^-$  solid solution  $[\text{Ca}_2\text{Al}(\text{OH})_6]^{+}[(\text{Cl})_{1-x}(\text{OH})_x(\text{H}_2\text{O})_{2+x}]^{-}$ , and the carbonate AFm phase and silicate AFm phase (strätlingite) are also known (Taylor 1973; von Hentschel and

\*E-mail: kirkpat@hercules.geology.uiuc.edu

†Current address: Korea Environment Institute, 1049-1 Sadang-Dong, Dongjak-Gu, Seoul, 156-090, Korea.

Kuzel 1976; Fischer et al. 1980; Passaglia and Sacerdoti 1988; Sacerdoti and Passaglia 1988)

The structures of both HT and AFm phases can be thought of as being based on those of simple hexagonal layered hydroxides such as brucite or portlandite (Terzis et al. 1987; Bellotto et al. 1996). Positive, permanent layer charge is developed by, e.g., Al for Mg or Ca substitution, resulting in incorporation of interlayer anions and associated water molecules. In hydrotalcite, the Al and Mg of the main hydroxide layer are disordered over one site but retain the sixfold coordination of Mg in brucite. The distribution of anions and water molecules in the interlayer space is, thus, disordered. In contrast, in hydrocalumite and other AFm phases for which structures are known (Allmann 1977; Terzis et al. 1987; Sacerdoti and Passaglia 1988), the Ca and Al are ordered in the hydroxide layer, and the interlayer water molecules are coordinated to the Ca atoms, creating sevenfold-coordinated Ca-sites. The localization of the interlayer water at the Ca-sites results in a well-ordered interlayer structure, which we show here yields better defined Cl<sup>-</sup> structural environments and a sharper structural phase transition than for HT.

### EXPERIMENTAL METHODS

Hydrotalcite was synthesized by mixing MgCl<sub>2</sub> and AlCl<sub>3</sub> solutions using the coprecipitation method of Miyata (1975). The sample used here was then recrystallized at 200 °C in a Parr bomb under autoclave conditions for 10 days. The solid sample was centrifugally separated from the solution, washed and vacuum filtered to remove excess surface Cl, dried at 70 °C for 24 hours, and stored in a dry nitrogen atmosphere. Chemical analysis by inductively coupled plasma (ICP) emission spectroscopy, titration and CHN analyzer (UIUC School of Chemical Sciences Microanalytical Lab) yields a structural formula of [Mg<sub>0.764</sub>Al<sub>0.236</sub>(OH)<sub>2</sub>][(CO<sub>3</sub>)<sub>0.007</sub>Cl<sub>0.221</sub> · nH<sub>2</sub>O]. This composition is in agreement with the nominal Mg/(Mg+Al) ratio but shows a small amount of carbonate, which is probably from exposure to the atmosphere. Powder XRD shows it to be phase-pure hydrotalcite. Its surface area obtained using BET methods is quite large, 31.2 m<sup>2</sup>/g.

The hydrocalumite was made by hydration of crystalline Ca<sub>3</sub>Al<sub>2</sub>O<sub>6</sub> in 1 M CaCl<sub>2</sub> solution at a solid/solution ratio of 1/100 at 40 °C for three days in a sealed N<sub>2</sub> atmosphere. The hydration product was washed and filtered with a millipore filter, dried over P<sub>2</sub>O<sub>5</sub> for 8 hours and stored in dry N<sub>2</sub>. Chemical analysis yields a structural formula of Ca<sub>1.96</sub>Al<sub>1.04</sub>(OH)<sub>6</sub>Cl<sub>0.76</sub>(CO<sub>3</sub>)<sub>0.14</sub> · 2.10H<sub>2</sub>O, in agreement with expectation. Powder X-ray diffraction shows it to be phase-pure. Its BET surface area is less than for our hydrotalcite, 3.9 m<sup>2</sup>/g.

These <sup>35</sup>Cl NMR spectra shown here were collected under static conditions at 48.99 MHz using a spectrometer equipped with a Tecmag Aries data system, Doty scientific and homebuilt probes, and an 11.7 T superconducting magnet. A two-pulse spin-echo pulse sequence with 16-step phase cycling was used (Kunwar et al. 1986) Spectra were collected at temperatures varying from +130 to -100 °C using a liquid nitrogen cooling system and a resistance heating system. For these spectra the sample container was covered loosely with Teflon sheet to prevent explosion by increased water pressure at elevated tem-

peratures. For spectra collected at room temperature and controlled relative humidity (R.H.), the samples were placed in an open glass tube, equilibrated for several days over saturated salt solutions (Lide 1998), sealed quickly with a stopper, and then with epoxy. Temperature was calibrated relative to the phase transition of hydrocalumite at 6 °C.

## RESULTS AND DISCUSSION

### Hydrocalumite

The <sup>35</sup>Cl NMR spectra for hydrocalumite are quite well resolved, as expected from its ordered Ca,Al distribution, and show substantial changes with changing temperature and relative humidity (Figs. 1 and 2). At room temperature and variable relative humidity, the spectra contain at least two components. The largest one is quadrupole dominated and contains the two maxima at 149 and -239 ppm. <sup>35</sup>Cl has spin *I* = 3/2 and a quadrupole moment of  $-7.89 \times 10^{-2}$  (units of 10<sup>-24</sup> cm<sup>2</sup>). Thus, quadrupolar effects on the line shape are expected for all but the most symmetrical unaveraged environments. This component is well simulated by a site with an isotropic chemical shift of 30 ± 5 ppm, a quadrupole coupling constant (QCC) of 2.87 MHz, and a nearly zero asymmetry parameter. This small asymmetry parameter indicates that the Cl<sup>-</sup> site is axially symmetric or nearly so under these conditions. Because of the quantitative dominance of this resonance, its lack of variation with

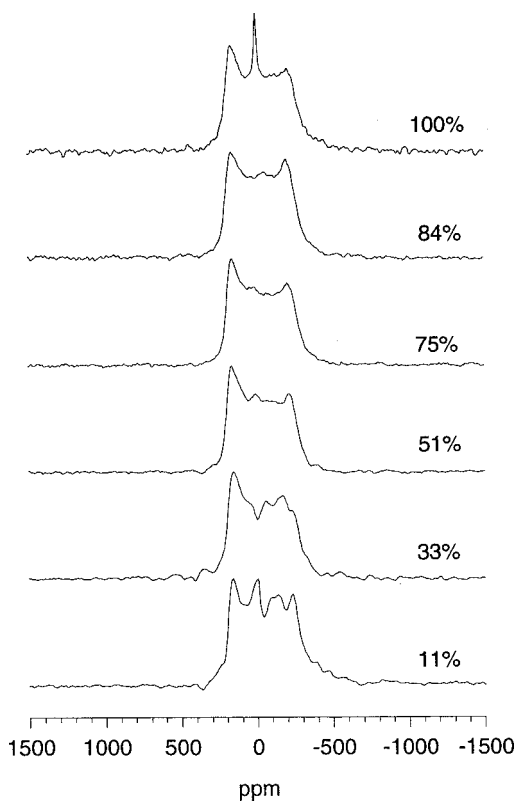
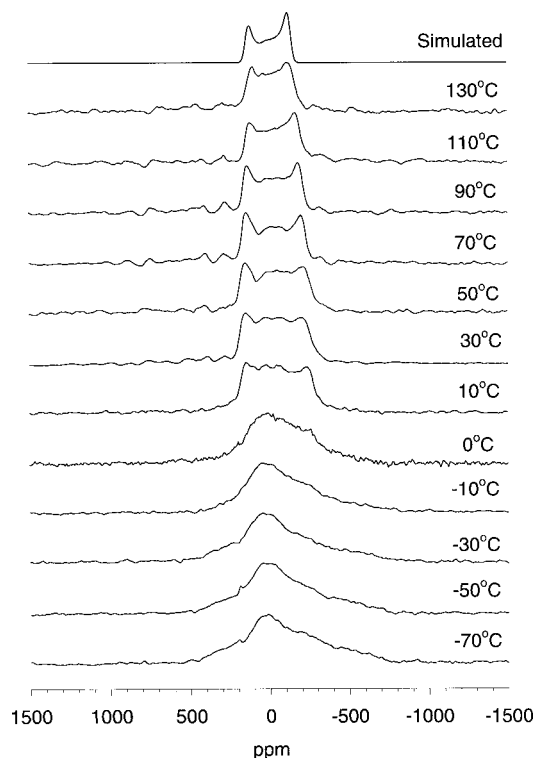


FIGURE 1. Static 48.991 MHz <sup>35</sup>Cl NMR spectra of hydrocalumite collected at room temperature and the indicated relative humidities (R.H.).



**FIGURE 2.** Static 48.99 MHz  $^{35}\text{Cl}$  NMR spectra of hydrocalumite collected at the indicated temperatures. The top spectrum is a single-site simulation of the observed 130°C spectrum; see text for parameters.

R.H., and the relatively small surface area of this sample, we interpret it to represent interlayer chloride. The smaller spectral component is more variable and is more difficult to characterize because of peak overlap. At low relative humidity there are multiple peaks in the central part of the spectrum and some additional intensity on the outside, consistent with quadrupolar contribution to the shape of this peak. With increasing relative humidity this component narrows, and at 100% R.H. it is quite narrow, indicating dynamical peak narrowing (see, e.g., Stebbins 1988, and Kim et al. 1996). This complex component probably represents surface chloride which takes on a progressively more symmetrical environment as the amount of surface water increases. Near 100% R.H. or with bulk solution present it becomes dynamically averaged with the surface or bulk water in a manner similar to Cs on illite surfaces (Kim and Kirkpatrick 1998b).

The elevated-temperature spectra (Fig. 2) are generally resemble the room temperature spectra above 10°C, but dramatic differences occur at lower temperatures. In the higher temperature range, the principle component is well simulated with a QCC that decreases from 2.87 MHz at 10°C to 2.22 MHz at 130°C, a temperature independent isotropic chemical shift of  $30 \pm 5$  ppm, and a temperature independent asymmetry parameter of zero. The simulation (Fig. 2, top) matches well the spectrum observed at 130°C. Again, the zero asymmetry parameter indicates axial or nearly axial symmetry. The smaller, central component disappears at higher temperatures, probably due to increased peak width caused by an increased QCC as the sur-

face water evaporates. Under these conditions, the signal is simply lost in the main peak. The singularities in these spectra are quite well defined, but a line broadening of 50 ppm is required for reasonable simulations.

Below 0°C the observed line shape is significantly different, and the bulk of the intensity is reasonably well simulated at all temperatures using a peak with a QCC of 3.0 MHz, an asymmetry parameter of 0.9, and an isotropic chemical shift of  $26 \pm 5$  ppm. This chemical shift does not significantly differ from that in the high-temperature phase. Other smaller components exist but are difficult to characterize due to peak overlap. Most importantly, the larger asymmetry parameter clearly indicates a change to a non-axially symmetric interlayer  $\text{Cl}^-$ -site.

DSC shows a sharp thermal anomaly near 6°C, indicative of a well-defined structural phase transition at this temperature (data not shown). At a heating/cooling rate of 10°C/minute, the peak is about 5°C wide at half height. On heating the onset of the peak occurs at  $4 \pm 3$ °C and on cooling at  $8 \pm 3$ °C, consistent with the change in the NMR asymmetry parameter.

Together, the NMR and DSC data suggest that there is a well defined, essentially first order phase transition near 6°C at which the symmetry at the  $\text{Cl}^-$  site changes from triaxial in the low-temperature phase to uniaxial or nearly so in the high-temperature phase. We interpret these results, in combination with X-ray structure refinement (Terzis et al. 1987), to indicate that this phase transition is of the dynamical order-disorder type, comparable in many ways to those of tridymite and cristobalite (Phillips et al. 1993 and references therein). In phase transitions of this type, atoms that are rigidly held in the low-temperature phase become mobile in the high-temperature phase. If this mobility occurs at a frequency greater than approximately 0.1 times the peak width, it causes changes in the NMR peak shape (called dynamical averaging; see, e.g., Stebbins 1988; Weiss et al. 1990; Kim et al. 1996). In structure refinements based on diffraction data, the thermal parameters for the atoms that are in motion are large. In hydrocalumite the thermal ellipsoids for the water molecules and chlorides are significantly larger than those of the Ca, Al and O sites of the hydroxide layer ( $0.0333$  to  $0.0646$  Å<sup>2</sup> vs.  $0.0104$  to  $0.0143$  Å<sup>2</sup>; Terzis et al. 1987) consistent with this interpretation. In the room temperature structure refinement of Terzis et al. (1987), the  $\text{Cl}^-$  is tenfold coordinated by H, forming a continuous hydrogen bonding network in the interlayer, but does not have uniaxial symmetry. The discrepancy between the XRD and NMR data can be reconciled by proposing that relative motion of the waters and  $\text{Cl}^-$  results in a time-averaged uniaxial symmetry. At 0°C, the thermal energy,  $RT$ , is 2.3 kJ/mol and becoming on the order of typical hydrogen bond strengths (10–20 kJ/mol). Thus, the onset of breaking and reforming hydrogen bonds is expected and is, indeed, observed at even lower temperatures for interlayer metals in smectites (e.g., Weiss et al. 1990).

The decrease in the  $^{35}\text{Cl}$  QCC with increasing temperature in the high-temperature phase also supports a dynamical interpretation. QCC is a measure of the electric field gradient at the observed nucleus, and in rigid crystal structures it is normally quite insensitive to temperature, as in the low-temperature hydrocalumite phase here or in the low-temperature phase of  $\text{AlPO}_4$  cristobalite (e.g., Phillips et al. 1993). In phases in which

there is dynamically averaging, such as analcime at elevated temperatures (Kim and Kirkpatrick 1998a), time averaged QCCs can change dramatically with varying temperature. In hydrocalumite, the dynamics in combination with the constraints of the structure leads to near uniaxial, rather than isotropic, symmetry.

Changes in NMR spectral shape require temporal fluctuations in the local structural environment (e.g., chemical shift or symmetry), which can result from either relative atomic motion at a site or site hopping. It is difficult to separate contributions from these effects. One possibility for hydrocalumite is that the uniaxial  $C_1$ -symmetry in the high-temperature phase is due to motion of the chlorides and water molecules in place (e.g., vibration, rotation, or libration), and that the decreasing QCC with increasing temperature is due to an increased rate of hopping among sites. Significant hydroxyl for chloride exchange occurs for our sample in 5 min at room temperature, indicating a relatively large diffusion coefficient and the possibility of rapid site exchange. In this model, the reduced (triaxial) symmetry in the low-temperature phase is due to the chloride ions and water molecules becoming locked into position or with their frequency of motion reduced to less than approximately 2 kHz ( $0.1\times$  the static peak width; see, e.g., Weiss et al. 1990). Low-temperature structure refinements and variable-temperature  $^1\text{H}$ ,  $^2\text{H}$ , and  $^{17}\text{O}$  NMR observation of the water molecules would provide confirming evidence of this interpretation.

To our knowledge these data are the first to strongly support a well-defined dynamical phase transition related to interlayer species in layered oxide materials with interlayer water (e.g., smectites or MMLHs). It occurs because the well-ordered structure of hydrocalumite allows the coordinated atomic motion required for such a phase transition (see, e.g., Salje 1990).

### Hydrocalumite

The  $^{35}\text{Cl}$  NMR spectra for hydrocalumite are less well resolved than those of the hydrocalumite and contain only one broad peak, which changes significantly with temperature (Fig. 3). These changes are best interpreted in terms of changing quadrupole coupling constant and asymmetry parameter, as for hydrocalumite. At  $-97$  and  $-80$  °C, the observed peak is featureless but skewed to the right indicating the presence of unaveraged quadrupolar line broadening. The peak at  $-80$  °C is narrower than at  $-97$  °C, suggesting the onset of detectable atomic motion. Because of the lack of singularities, spectral simulation is difficult, but the broadest components have a QCC of about 2.4 MHz, and all reasonable fits require a large asymmetry parameter approaching 1. At  $-61$  °C the peak is even narrower and less skewed to the right. Between  $-40$  °C and room temperature, the peak has an unusual flat-topped shape that is best interpreted as a quadrupole-dominated peak with significant disorder. The squared shape indicates a low asymmetry parameter (approaching zero), as for the high-temperature phase of hydrocalumite. The QCCs of the components that are related to the edges of the flat top decrease with increasing temperature from about 1.5 MHz at  $-40$  °C to about 1.2 MHz at room temperature.

The flat-topped spectra can be understood in terms of a

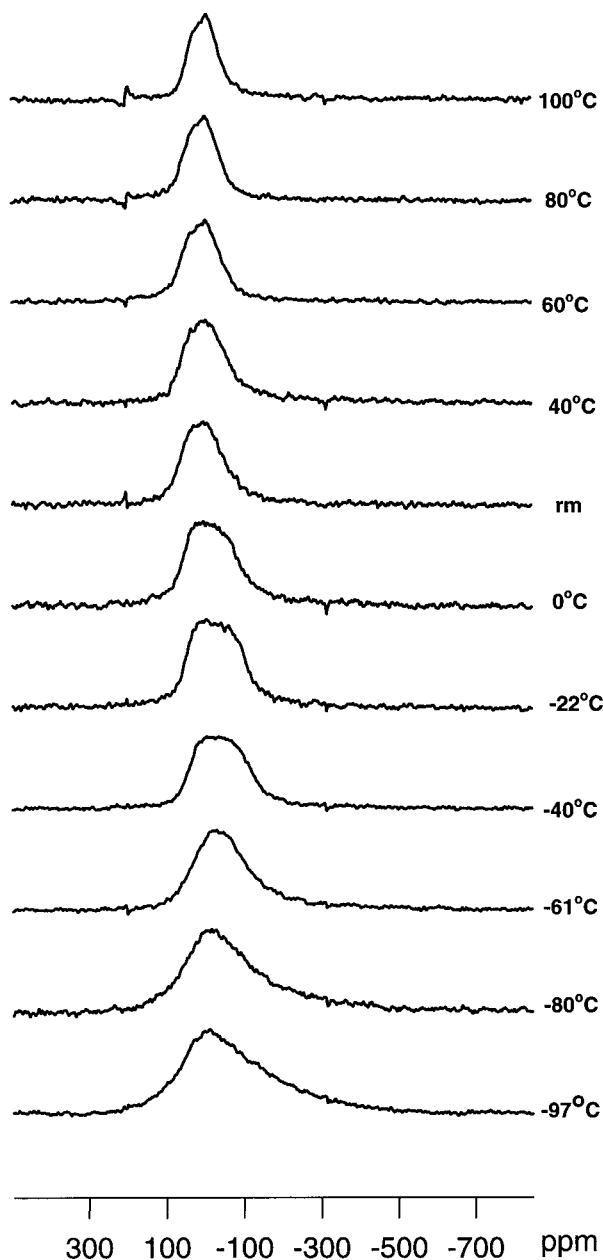


FIGURE 3. Static 48.99 MHz  $^{35}\text{Cl}$  NMR spectra of hydrocalumite collected at the indicated temperatures.

dominant site with a QCC of 1.2–1.5 MHz and an asymmetry parameter close to zero along with other components with larger and smaller QCCs. These other components add to the width and fill in between the singularities, such as those observed for hydrocalumite (Figs. 1 and 2). We have observed such spectra for hydrocalumite with mixed  $\text{Cl}^-$  and  $\text{OH}^-$  in the interlayer (data not shown). Many of the less well-defined sites are probably on the surface, because this sample has a specific surface area almost 10 times that of the hydrocalumite. The disordered  $\text{Mg,Al}$  distribution in the main hydroxide layer may also contribute. Above  $40$  °C the peaks are less obviously flat-topped,

and the weak singularity near  $-9$  ppm suggests some quadrupole contribution to the peak. The width suggests a QCC of about 1.0 MHz at  $100^\circ\text{C}$ . In contrast to the simulations for hydrocalumite, the poor resolution of these spectra requires line broadening of about 90 ppm for reasonable fits at most temperatures, although it decreases to about 50 ppm at  $100^\circ\text{C}$ . Much of this line broadening must be due to the presence of  $\text{Cl}^-$  on surface and interlayer sites with different chemical shifts and quadrupolar parameters. Line broadening due to  $^1\text{H}$ - $^{35}\text{Cl}$  dipolar coupling should be at most about 30 ppm for an inter-nuclear H-Cl distance of  $2 \text{ \AA}$ , and this broadening is reduced by any reorientational molecular motion.

DSC data (not shown) for the recrystallized hydrotalcite sample show a weak thermal anomaly centered at  $-85^\circ\text{C}$  on increasing temperature. In contrast to hydrocalumite, it is about  $25^\circ\text{C}$  broad. The low temperature of these thermal effects is consistent with the observed changes in the  $^{35}\text{Cl}$  NMR spectra in this temperature range.

The change in the  $^{35}\text{Cl}$  quadrupole asymmetry parameter from near 1 at the lowest temperatures to near 0 at about  $-40^\circ\text{C}$ , in combination with the observed broad DSC anomaly, suggests that Cl-hydrotalcite undergoes a dynamical order-disorder structural phase transition similar to hydrocalumite, but that this transition occurs at a lower temperature and is spread over a larger temperature interval. The broader temperature interval for the transition is expected from the disordered distributions of octahedral Mg and Al and interlayer waters and chloride. Disorder causes the motions of the interlayer species to be less well coordinated than in hydrocalumite, causing changes in the frequencies of these motions and the phase transition to be spread over a considerable temperature range. This difference is comparable to the effects of structural and compositional disorder on the dynamical  $\alpha$ - $\beta$  phase transition of cristobalite (Thomas et al. 1994) and Al,Si or Ca,Na disorder on the  $P\bar{1}$ - $I\bar{1}$  transition in anorthite-rich feldspars (Redfern 1992; Phillips and Kirkpatrick 1995 and references in these papers). The origin of the lower transition temperature for hydrotalcite compared to hydrocalumite is unclear, because of the compositional differences between the phases. It does, however, parallel the behavior observed for ordered vs. disordered cristobalite and anorthite, suggesting that the well-ordered interlayer  $\text{Cl}_2\text{H}_2\text{O}$  distribution of hydrocalumite helps stabilize its structure. Study of the effect of the variable Mg,Al ratio in hydrotalcite would help clarify this issue.

#### ACKNOWLEDGMENTS

This research was supported by NSF grant no. EAR95-26317 (R.J.K., P.I.) and the NSF Science and Technology Center for Advanced Cement-Based Materials. Andrey Kalinichev provided useful discussion concerning hydrogen bonded systems.

#### REFERENCES CITED

- Allmann, R. (1977) Refinement of the hybrid layer structure  $[\text{Ca}_2\text{Al}(\text{OH})_6]^{+1/2}(\text{SO}_4)_2 \cdot 3\text{H}_2\text{O}$ . *Neues Jahrbuch für Mineralogie Monatshefte*, 1977, 136-143.
- Amin, S. and Jayson, G.G. (1996) Humic substance uptake by hydrotalcites and PILCS. *Water Resources*, 30, 299-306.
- Bellotto, M., Rebours, B., Clause, O., Lynch, J., Bazin, D., and Elkaiem, E. (1996) A reexamination of hydrotalcite crystal chemistry. *Journal of Physical Chemistry*, 100, 8527-8534.
- Fischer, R., Kuzel, H.-J., and Schellorn, H. (1980) Hydrocalumite: Mischkristalle von "Friedelschem Salz"  $3\text{CaO} \cdot \text{Al}_2\text{O}_3 \cdot \text{CaCl}_2 \cdot 10\text{H}_2\text{O}$  und Tetracalciumaluminat-hydrat  $3\text{CaO} \cdot \text{Al}_2\text{O}_3 \cdot \text{Ca}(\text{OH})_2 \cdot 12\text{H}_2\text{O}$ . *Neues Jahrbuch für Mineralogie Monatshefte*, 1980, 322-334.
- Hermosin, M.C., Pavlovic, I., Ulibarri, M.A., and Cornejo, J. (1996) Hydrotalcite as sorbent for trinitrophenol: sorption capacity and mechanism. *Water Resources*, 30, 171-177.
- Kim, Y. and Kirkpatrick, R.J. (1998a) High-temperature multi-nuclear NMR investigation of analcime. *American Mineralogist*, 83, 339-347.
- (1998b) NMR  $T_1$  relaxation study of  $^{133}\text{Cs}$  and  $^{23}\text{Na}$  adsorbed on illite. *American Mineralogist*, 83, 661-665.
- Kim, Y., Kirkpatrick, R.J., and Cygan, R.T. (1996)  $^{133}\text{Cs}$  NMR study of cesium on the surfaces of kaolinite and illite. *Geochimica Cosmochimica Acta*, 60, 4059-4074.
- Kunwar, A.C., Turner, G.L., and Oldfield, E. (1986) Solid-state spin-echo Fourier transform NMR of  $^{39}\text{K}$  and  $^{69}\text{Zn}$  salts at high field. *Journal of Magnetic Resonance*, 69, 124-127.
- Lide, D.R. (1998) CRC Handbook of Chemistry and Physics, 79th Edition. CRD Press, p. 15-25.
- Marcelin, G., Stockhausen, N.J., Post, J.F.M., and Schutz, A. (1989) Dynamics and ordering of interlayered water in layered metal hydroxides. *Journal of Physical Chemistry*, 93, 4646-4650.
- Miyata, S. (1975) The synthesis of hydrotalcite-like compounds and their structures and physico-chemical properties-I. *Clays and Clay Minerals*, 23, 369-375.
- (1983) Anion-exchange properties of hydrotalcite-like compounds. *Clays and Clay Minerals*, 31, 305-311.
- Olguin, M.T., Bosch, P., Acosta, D., and Bulbulian, S. (1998)  $^{131}\text{I}$  sorption by thermally treated hydrotalcites. *Clays and Clay Minerals*, 46, 567-573.
- Parker, L.M., Milestone, N.B., and Newman, R.H. (1995) The use of hydrotalcite as an anion absorbent. *Industrial Engineering and Chemical Research*, 34, 1196-1202.
- Passaglia, E. and Sacerdoti, M. (1988) Hydrocalumite from Monalto di Castro, Viterbo, Italy. *Neues Jahrbuch für Mineralogie Monatshefte* 1988, 454-461.
- Phillips, B.L. and Kirkpatrick, R.J. (1995) High-temperature  $^{29}\text{Si}$  MAS NMR spectroscopy of anorthite ( $\text{CaAl}_2\text{Si}_2\text{O}_8$ ) and its P1-I1 phase transition. *Physics and Chemistry of Minerals*, 22, 268-278.
- Phillips, B.L., Thompson, J.G., Xiao, Y., and Kirkpatrick, R.J. (1993) Constraints on the structure and dynamics of the  $\beta$ -cristobalite polymorphs of  $\text{SiO}_2$  and  $\text{AlPO}_4$  from  $^{31}\text{P}$ ,  $^{27}\text{Al}$  and  $^{29}\text{Si}$  NMR spectroscopy to 770K. *Physics and Chemistry of Minerals*, 20, 341-352.
- Pinnavaia, T.J. (1995) Clay catalysts: opportunities for use in improving environmental quality. *Clays Controlling Environment. Proceedings of the 10th International Clay Conference, Commonwealth Scientific and Industrial Research Organization, East Melbourne, Australia.*
- Redfern, S.A.T. (1992) The effects of Al, Si disorder on the I1-P1 co-elastic phase transition of Ca-rich plagioclase. *Physics and Chemistry of Minerals*, 19, 246-254.
- Sacerdoti, M. and Passaglia, E. (1988) Hydrocalumite from Latium, Italy: its crystal structure and relationship with related synthetic phases. *Neues Jahrbuch für Mineralogie Monatshefte*, 1988, 462-475.
- Salje, E.K.H. (1990) Phase transitions in ferroelastic and co-elastic crystals, 366 p. Cambridge University Press, Cambridge, U.K.
- Stebbins, J.F. (1988) NMR spectroscopy and dynamic processes in mineralogy and geochemistry. *Mineralogical Society of America, Reviews in Mineralogy*, 18, 405-429.
- Taylor, H.F.W. (1973) Crystal structures of some double hydroxide minerals. *Mineralogical Magazine*, 39, 377-389.
- (1997) *Cement chemistry*, 2nd ed. Thomas Telford Publishing, London.
- Terzis, A., Filippakis, S., Kuzel, H.-J., and Burzlaff, H. (1987) The crystal structure of  $\text{Ca}_2\text{Al}(\text{OH})_6\text{Cl} \cdot 2\text{H}_2\text{O}$ . *Zeitschrift für Kristallographie*, 181, 29-34.
- Thomas, E.S., Thompson, J.G., Withers, R.L., Sterns, M., Xiao, Y., and Kirkpatrick, R.J. (1994) Further investigation of the stabilization of  $\beta$ -cristobalite. *Journal of the American Ceramic Society*, 77, 49-56.
- Ulibarri, M.A., Pavlovic, I., Hermosin, M.C., and Cornejo, J. (1995) Hydrotalcite-like compounds as potential sorbents of phenols from water. *Applied Clay Science*, 10, 131-45.
- van der Pol, A., Mojet, B.L., van de Ven, E., and de Boer, E. (1994) Ordering of intercalated water and carbonate anions in hydrotalcite. an NMR study. *Journal of Physical Chemistry*, 98, 4050-4054.
- von Hentschel, G. and Kuzel, H.-J. (1976) Strätlingit,  $2\text{CaO} \cdot \text{Al}_2\text{O}_3 \cdot \text{SiO}_2 \cdot 8\text{H}_2\text{O}$ , a new mineral. *Neues Jahrbuch für Mineralogie Monatshefte*, 1976, 326-330.
- Wada, S.-I. and Masuda, K. (1995) Control of salt concentration of soil solution by the addition of synthetic hydrotalcite. *Soil Science and Plant Nutrition (Tokyo)*, 41, 377-381.
- Weiss, C.A. Jr., Kirkpatrick, R.J., and Altaner, S.P. (1990) The structural environments of cations adsorbed onto clays:  $^{133}\text{Cs}$  variable-temperature MAS NMR spectroscopy of hectorite. *Geochimica Cosmochimica Acta*, 54, 1655-1669.

MANUSCRIPT RECEIVED SEPTEMBER 28, 1998

MANUSCRIPT ACCEPTED MARCH 16, 1999

PAPER HANDLED BY JONATHAN F. STEBBINS